

# CDMSlite Run 3 Data Release

SuperCDMS Collaboration

June 2020

This document accompanies the public release of the CDMSlite Run 3 data and gives explanatory material related to the released files themselves and their use in reproducing published upper limit results. The WIMP-search results from these data are found in <https://arxiv.org/abs/1808.09098> [1]. All experimental data required for DM searches are included in the release. Background models that are not explicitly defined in Ref. [1] are also provided. The provided data and information allows the community to use this release for their own analyses or for reproducing the CDMSlite Run 3 results.

The provided experimental and supplemental data files and information are described in Sec. 1. The upper limit on WIMP-nucleon interactions was calculated using a profile likelihood fit, as described in Ref. [1] and Sec. 2.

## 1 Description of the Files

Seven text (.txt) files accompany this data release and can be found in the `data.files` directory of the accompanying .zip file. The names and descriptions of these files are

- **event\_EnergykeVee\_Per#.txt**: These files contain a column of event energies in units of keV<sub>ee</sub>. The ‘#’ in the file name is a placeholder for ‘1’ or ‘2,’ indicating the corresponding measurement period (Period 1 or Period 2). The 208 events from Period 1 and 193 events from Period 2 are those from the final CDMSlite Run 3 spectrum used to compute WIMP-search limits. The energy range used in the WIMP-search results is 0.07 to 2 keV<sub>ee</sub>. The spectrum generated by combining the events in Period 1 and Period 2 is given in Fig. 1. The spectrum can be reproduced by using 10 eV<sub>ee</sub> sized bins with the lowest energy bin spanning 0-10 eV<sub>ee</sub>.
- **efficiency\_parametrization\_keVee.txt** The WIMP-search efficiency parametrization is given by

$$h(E; \vec{\mu}_e) = \mu_{e_1} \times \left[ 1 + \operatorname{erf} \left( \frac{E - \mu_{e_2}}{\sqrt{2}\mu_{e_3}} \right) \right]. \quad (1)$$

Central values for and covariances between the  $\vec{\mu}_e$  parameters are provided in the file. Figure 2 shows the resulting signal efficiency as a function

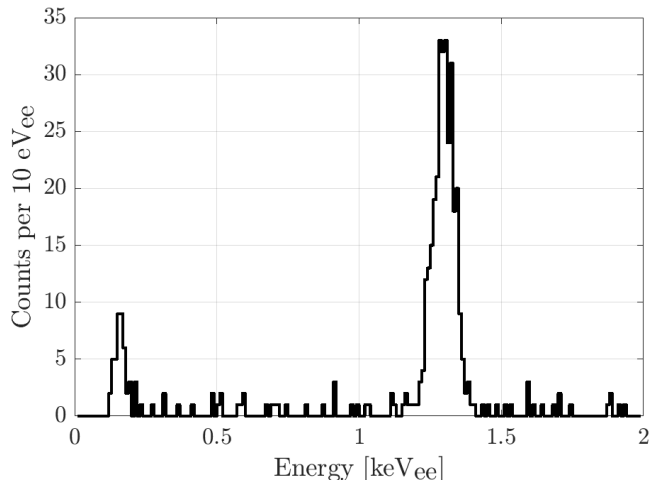


Figure 1: Energy spectrum of the CDMSlite Run 3 data, with Period 1 and Period 2 combined, between  $0.07 \text{ keV}_{ee}$  and  $2 \text{ keV}_{ee}$ .

of energy, with energy defined over the  $0.07$  to  $2 \text{ keV}_{ee}$  range used in the WIMP-search results. The  $\pm 1\sigma$  uncertainty band, derived from the provided covariance matrix between  $\vec{\mu}_e$  parameters, is also shown.

- **resolution\_parametrization\_keVee.txt** The CDMSlite detector energy resolution parametrization is given by

$$\sigma_T(E_{r,ee}) = \sqrt{\sigma_E^2 + BE_{r,ee} + (AE_{r,ee})^2}. \quad (2)$$

Central values for the  $\sigma_E$ ,  $B$ , and  $A$  parameters are provided for Period 1 and Period 2. The  $\sigma_E$  and  $B$  parameters are in units of  $\text{keV}_{ee}$ . The covariances between the  $\sigma_E$ ,  $B$ , and  $A$  parameters are also provided.

- **surface\_background\_distributions\_keVee.txt** This file contains the distributions for the three surface backgrounds: the copper directly above the detector, the cylindrical housing, and the surface of the germanium crystal itself. The first column consists of energies between  $0$  and  $2 \text{ keV}_{ee}$ . The later columns consist of the surface background distributions in units of event density ( $\frac{\text{events}}{\text{keV}_{ee}}$ ). In addition to the nominal event density distribution ( $\rho_0$ ), the upper ( $\rho_+$ ) and lower ( $\rho_-$ ) densities are provided. The columns are organized as follows:

- Columns 2-4:  $\rho_-$ ,  $\rho_0$ , and  $\rho_+$  distribution for copper directly above the detector during Period 1
- Columns 5-7:  $\rho_-$ ,  $\rho_0$ , and  $\rho_+$  distribution for copper directly above the detector during Period 2

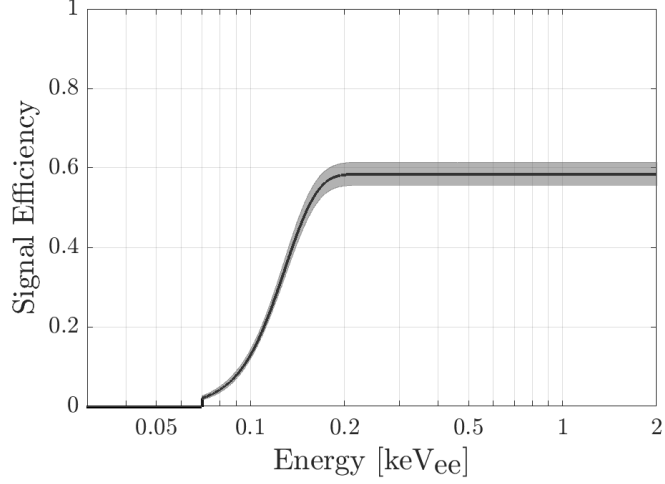


Figure 2: Signal efficiency and  $\pm 1\sigma$  uncertainty band between 0.07 keV<sub>ee</sub> and 2 keV<sub>ee</sub>.

- Columns 8-10:  $\rho_-$ ,  $\rho_0$ , and  $\rho_+$  distribution for the cylindrical housing during Period 1
- Columns 11-13:  $\rho_-$ ,  $\rho_0$ , and  $\rho_+$  distribution for the cylindrical housing during Period 2
- Columns 14-16:  $\rho_-$ ,  $\rho_0$ , and  $\rho_+$  distribution for the Germanium crystal surface during Period 1
- Columns 17-19:  $\rho_-$ ,  $\rho_0$ , and  $\rho_+$  distribution for the Germanium crystal surface during Period 2

Figure 3 shows the  $\rho_-$ ,  $\rho_0$ , and  $\rho_+$  distributions for the three surface backgrounds for Period 1 and Period 2.

- **morphing\_parameter\_constraints.txt** Central values for and covariances between the morphing parameters ( $m_1$ ,  $m_2$ , and  $m_3$ ) are provided in the file.
- **limit\_SI\_GeVc2\_cm2.txt** This file contains the published spin-independent WIMP-nucleon 90% CL upper limit. The first column contains WIMP-masses in units of GeV/ $c^2$ . The second column contains the limit values in units of cm<sup>2</sup>. This limit is shown in Fig. 4.

## 2 Limit Setting

The profile likelihood fit and method to calculate the WIMP-signal upper limit are described in Ref. [1]. In addition to the information provided in the files

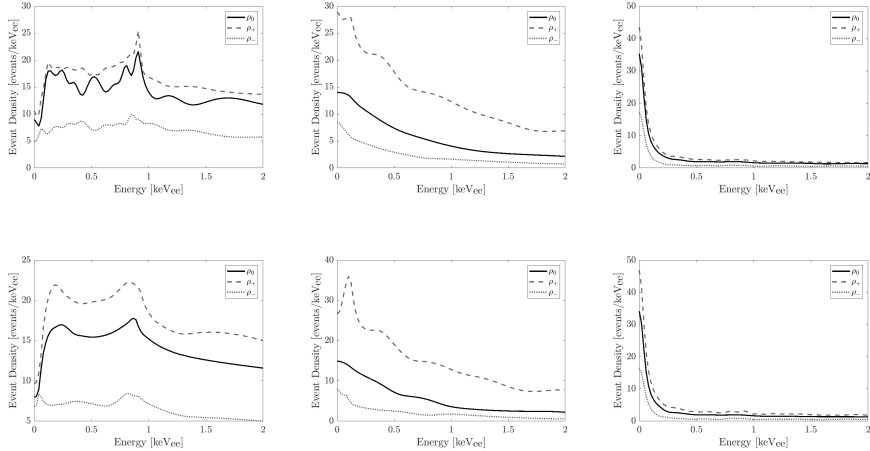


Figure 3: The  $\rho_-$ ,  $\rho_0$ , and  $\rho_+$  distribution for (left) the copper directly above the detector, (center) the cylindrical housing, and (right) the Germanium crystal surface. The top row distributions are for Period 1 and the bottom row distributions are for Period 2.

described above, the non-surface background models described in Ref. [1], and the WIMP-signal model derived in Ref. [2] using the Helm nuclear form factor in Ref. [3], are necessary to perform the likelihood fit. The exposures for Period 1 and Period 2 are 18.8 kg-day and 17.5 kg-day, respectively.

In order to convert the WIMP-signal shape from the  $\text{keV}_{\text{nr}}$  to the  $\text{keV}_{\text{ee}}$  energy scale, the average detector currents for Period 1 and Period 2 are  $87.5 \times 10^{-9}$  Amps and  $9.1 \times 10^{-9}$  Amps, respectively. The average detector current values allow the user to convert between energy scales using the information given in Sec. 2 of Ref. [1]. Specifically, the relationship between  $I_{\text{HV}}$  and the detector voltage ( $V_{\text{det}}$ ) is given in Eq. 6 in Ref. [1]. The conversions between energy scales, which depend on the detector voltage, are given by Eq. 3 and Eq. 4 in Ref. [1].

## References

- [1] R. Agnese, T. Aralis, T. Aramaki, I. J. Arnquist, E. Azadbakht, W. Baker, S. Banik, D. Barker, D. A. Bauer, T. Binder, M. A. Bowles, P. L. Brink, R. Bunker, B. Cabrera, R. Calkins, R. A. Cameron, C. Cartaro, D. G. Cerdeño, Y.-Y. Chang, J. Cooley, B. Cornell, P. Cushman, F. De Brienne, T. Doughty, E. Fascione, E. Figueroa-Feliciano, C. W. Fink, M. Fritts, G. Gerbier, R. Germond, M. Ghaith, S. R. Golwala, H. R. Harris, N. Herbert, Z. Hong, E. W. Hoppe, L. Hsu, M. E. Huber, V. Iyer, D. Jardin, A. Jastram, C. Jena, M. H. Kelsey, A. Kennedy, A. Kubik, N. A. Kurin

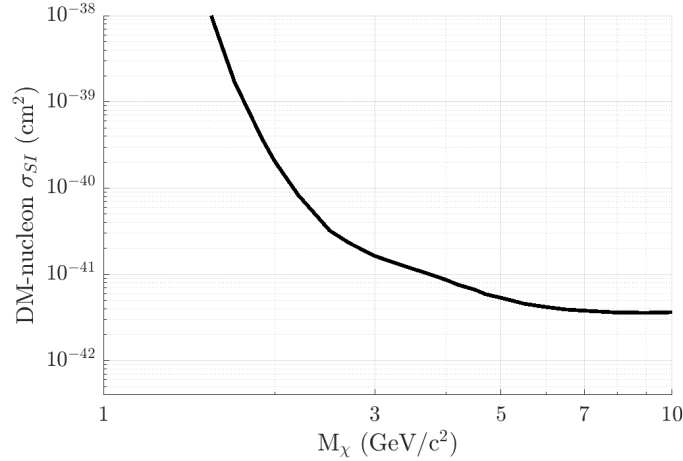


Figure 4: The CDMSlite Run 3 WIMP-nucleon cross section 90% CL upper limit.

sky, R. E. Lawrence, B. Loer, E. Lopez Asamar, P. Lukens, D. MacDonell, R. Mahapatra, V. Mandic, N. Mast, E. Miller, N. Mirabolfathi, B. Mohanty, J. D. Morales Mendoza, J. Nelson, H. Neog, J. L. Orrell, S. M. Oser, W. A. Page, R. Partridge, M. Pepin, F. Ponce, S. Poudel, M. Pyle, H. Qiu, W. Rau, A. Reisetter, R. Ren, T. Reynolds, A. Roberts, A. E. Robinson, H. E. Rogers, T. Saab, B. Sadoulet, J. Sander, A. Scarff, R. W. Schnee, S. Scorza, K. Senapati, B. Serfass, D. Speller, C. Stanford, M. Stein, J. Street, H. A. Tanaka, D. Toback, R. Underwood, A. N. Villano, B. von Krosigk, S. L. Watkins, J. S. Wilson, M. J. Wilson, J. Winchell, D. H. Wright, S. Yellin, B. A. Young, X. Zhang, and X. Zhao. Search for low-mass dark matter with cdmslite using a profile likelihood fit. *Phys. Rev. D*, 99:062001, Mar 2019.

- [2] J.D. Lewin and P.F. Smith. Review of mathematics, numerical factors, and corrections for dark matter experiments based on elastic nuclear recoil. *Astropart. Phys.*, 6(1):87–112, dec 1996.
- [3] Richard H. Helm. Inelastic and elastic scattering of 187-mev electrons from selected even-even nuclei. *Phys. Rev.*, 104:1466–1475, Dec 1956.